FRAGMENTATION OF BLOCKS: POSSIBLE RELATIONSHIP WITH EXPOSURE TIME BASED ON LROC NAC. O. Ruesch[1], E. Sefton-Nash[1], J. L. Vago[1], M. Kueppers[2], K. Krohn[3], K. Otto[3], [1]ESA/ESTEC, Keplerlaan 1, 2201 AZ, Noordwijk, The Netherlands (ottaviano.ruesch@esa.int). [2]ESA/ESAC, Villanueva de la Canada, Spain. [3]DLR, Institute for Planetary Research, Berlin, Germany.

Introduction: At a small spatial scale (<1 km), most of the rocky planetary surfaces can be described in morphological terms with three endmembers: bedrock, block, and fine regolith particles. These endmembers represent successive evolutionary stages of the surface. The understanding of the processes that link them genetically is fundamental to answer a variety of science questions, in particular for local, in situ investigation by robotic missions [1-3].

Blocks are usually produced from bedrock by mass wasting and impact cratering [e.g. 4]. Once formed, blocks are subject to a variety of effects that produce smaller fragments and eventually fine regolith material [e.g., 5,6]. The causes of these effects have been identified, e.g., micrometeorite bombardment and thermal fatigue, but how exactly the comminution process works on different planetary bodies remains largely to be investigated [7,8]. In the literature, several properties of blocks have been investigated [e.g. 4,9,10,11,12]. There is one aspect that has received very little attention: in situ fragmentation and formation of block clusters [13,14]. Here we refer to the clusters formed by fragmentation or erosion in place and not as fields of ejecta blocks or rock fall deposits.

Approach: We define the unambiguous identification of an in situ breakdown of a block with the observation of a fracture that splits, in planar view, parallel facets of two or more fragments, i.e., the fracture planes are parallel. In the cases where the fracture width is similar to or exceed the width of the largest fragment and the facets are not parallel, the genetic link is determined by the presence of loose material (fillet) and smaller fragments in a juxtaposed configuration.

We first searched for evidence of in situ fragmentation of boulders in the size range 5-100 meters in a variety of geologic context and bodies. Then, we investigated the morphologies of clusters on the rim of few lunar impact craters for which absolute model ages have been determined, as used in [5]. We used LROC NAC images down to 0.5 meter/pixel at low and high illumination angles and east and west directions. For a quantitative estimate of the clustering of each splitted block, we measured the distance *d* between the largest (primary) and second largest (secondary) fragment, normalized to the major axis lengths *L* of the fragments $p=2d/(L_{primary}+L_{secondary})$. High p values correspond to more fractured, and thus more loosely packed clusters. More complex spatial statistical measurements (e.g., area covered by all fragments) are currently hampered by the complex morphologies and shadows. This measurements was performed for about 15 clusters at each crater.

Preliminary Results: *Diversity of contexts.* Local breakdown is found for (i) blocks on the rim of lunar impact craters originally emplaced as ejecta boulders, (ii) blocks on slopes (e.g., Posidonius rille) and (iii) on crater floors originally formed by mass wasting, (iv) blocks on 433 Eros originally emplaced as ejecta boulders, and (v) blocks on 25143 Itokawa emplaced by reaccumulation, among others.

General remarks at lunar craters. Only a fraction of all identifiable large blocks (10-100 meters) are fractured. General morphological and morphometrical trends (Figure 1, left, and 2) are observed with the age of the craters and are reported further below. The morphologies found at a given crater are also found at craters of younger ages. In addition, there is a type of cluster morphology consistently present at each crater with many (>10) fragments. We did not include this type in the morphometry measurements because of the small size of the primary and/or secondary fragment (Figure 1, right).

Giordano Bruno (4±1.2 Ma). Blocks are mostly fractured with the fragments closely packed and of similar sizes. Blocks can also be composed of a primary fragment with few smaller fragments juxtaposed to one of its side. Identification of fractured blocks is more challenging at this young crater due to a high abundance of ejecta blocks.

Tycho (85 -18/+15 Ma). Qualitatively, blocks are relatively more fractured than at Giordano Bruno. Where occurring, smaller fragments are juxtaposed on one or two side of the primary fragment. Loose material (fillet) can be observed on the sides of the primary fragment.

Aristarcus (175 -9.1/+8.8 Ma). Although the morphologies are broadly similar to those of Tycho, in large clusters the perimeter of the primary fragment is partly surrounded by smaller fragments.

Copernicus (797 -52/+51 Ma). The perimeter of the largest fragment is mostly or completely juxtaposed by fine material (fillet) or fragments. The mean width of the largest fragment is smaller than the initial block size as inferred from the area covered by fragments. Loose material (fillet) develops into small scale talus around the fragments. Small fragments can be seen partly embedded in the talus.

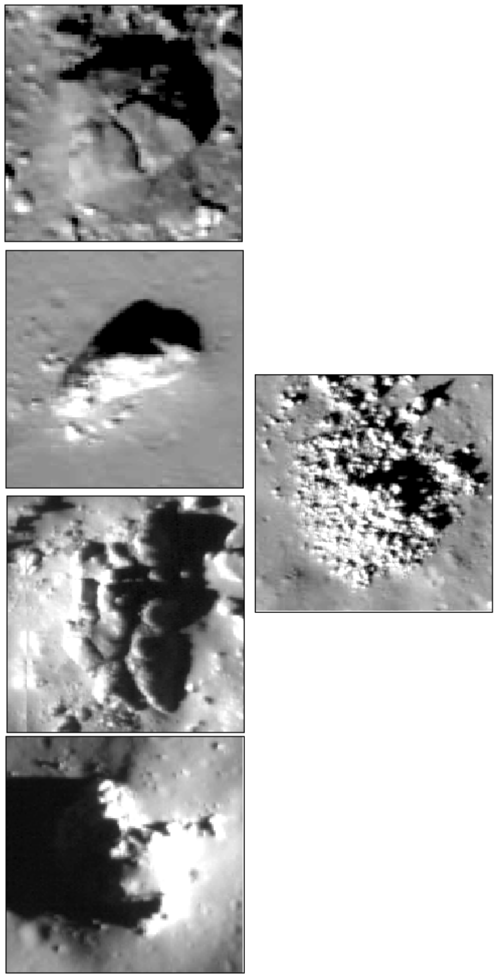

Figure 1. Example of blocks fragmented in situ. On the left, from top to bottom: crater Giordano Bruno, Tycho, Aristarcus and Copernicus, with image width 100 m, 100 m, 180 m, and 160 m, respectively. On the right an example of a different type of cluster observed at all craters, image width of 170 m.

Discussion: The processes leading to cluster formation can be grouped in two. (1) Fragmentation during emplacement, either at the moment of impact for ejecta blocks [15] or at the moment of a halt for downslope rolling blocks [16], and (2) fragmentation as a function of exposure time after emplacement.

Although processes belonging to both groups could play a role in eroding blocks, the morphological and morphometrical trends observed on lunar craters of different ages and the ubiquitous occurrence of rock breakdown on a variety of planetary bodies seem to suggest that the major factors controlling fragmentation are related to the exposure time and the original rock cohesion. The possible processes are: small high-velocity impactor/catastrophic rupture [e.g., 15], thermal fatigue [e.g., 13] and seismic shaking [e.g., 13,17].

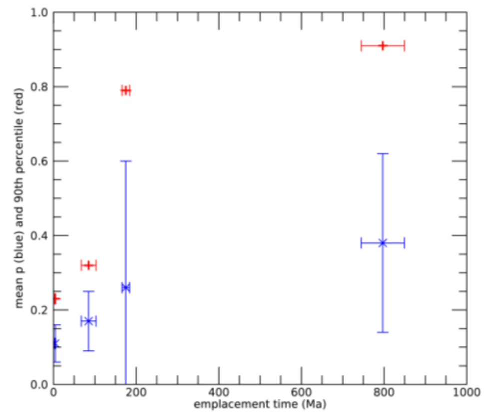

Figure 2. Plot of morphometric parameters of block clusters as a function of crater age from crater size-frequency distributions [5]. The error bars on mean p is the standard deviation σ. The 90th percentile (red) is the threshold separating the highest 10% of p values from the lower 90%.

The sequence of morphologies in Figure 1 is similar to the observations on Itokawa [14], where clusters of different degree of destruction by small high-speed impactor are reported. Here we suggest that there is a progressive destruction with exposure time and that it is due to an increase in the number of impactors and/or increase in their impact energy (e.g., sizes). The relative role of small high-velocity impactors and micrometeoroid abrasion through time remains to be determined.

Conclusions: Preliminary results suggest that morphology and morphometry of blocks fractured in situ are related to their emplacement time and reflect the degree of comminution. These results will be used to constrain the origin of rock-rich regions, e.g., Tsiolkovskiy crater [18], and to provide additional estimates for erosion rate on the lunar surface.

References: [1] Sefton-Nash et al., (2018) LPSC 49th, #2740. [2] Vago et al., (2017) Astrobiology, 17, 471-510. [3] Michel et al., (2018) LPSC 49th, #1144. [4] Kueppers et al., (2012) PSS, 66, 71-78. [5] Ghent et al., (2014) Geology, doi:10.1130/G35926.1. [6] Basilevesky et al., (2015) PSS, 117, 312-328. [7] Delbo et al., (2014) Nature, doi:10.1038/nature13153. [8] Molaro et al., (2017) Icarus, 294, 247-261. [9] Golombek et al., (2008) JGR, 113, E00A09. [10] Di et al., (2016) PSS, 120, 103-112. [11] Bart and Melosh, (2010) Icarus, 209, 337-357. [12] Schulzeck et al., (2018) PSS, 153, 142-156. [13] Dombard et al., (2010) Icarus, 210, 713-721. [14] Nakamura et al., (2008) EPS, 60, 7-12. [15] Robinson et al., (2002) MAPS, 37, 1651-1684. [16] Apollo 17 : Prelim. Sci. Rep.t, (1973) NASA SP-330. [17] Quade et al., (2012) Geology, 40, 851-854. [18] Greenhagen et al., (2016) Icarus, 273, 237-247.